Available online at www.sciencedirect.com

ScienceDirect

Energy Procedia 124 (2017) 464–469

Energy Procedia

www.elsevier.com/locate/procedia

7th International Conference on Silicon Photovoltaics, SiliconPV 2017

Thermomechanical stress analysis of PV module production processes by Raman spectroscopy and FEM simulation

Andreas J. Beinert[a,b,*], Pascal Romer[a], Andreas Büchler[a], Viola Haueisen[a], Jarir Aktaa[b], Ulrich Eitner[a]

[a]*Fraunhofer Institute for Solar Energy Systems ISE, Heidenhofstraße 2, 79110 Freiburg, Germany*
[b]*Karlsruhe Institute of Technology (KIT), Institute for Applied Materials, Hermann-von-Helmholtz-Platz 1, 76344 Eggenstein-Leopoldshafen, Germany*

Abstract

Raman spectroscopy is used for measuring stress in microelectronic devices [1] as well as in solar cells [2, 3]. However, on PV module level it has not been examined yet. We transfer the method in order to enable the experimental determination of thermomechanical stress in PV modules. For this purpose the stress in non-soldered, soldered and laminated solar cells is measured by a confocal Raman spectrometer. Additionally we simulate the thermomechanical stress induced by soldering and lamination by finite element modelling. Considering the initial stress state of the solar cells and a linear elastic material model of EVA, the results show a good agreement. By Raman spectroscopy we find the compressive stress in the solar cell after lamination to add up to 53 ± 6 MPa.

Peer review by the scientific conference committee of SiliconPV 2017 under responsibility of PSE AG.

Keywords: Mechanical stress measurement; Raman spectroscopy; Module production; FEM, Thermomechanics

* Corresponding author. Tel.: +49 (0)761/ 4588-5630; fax: +49 (0)761/ 4588-9630.
E-mail address: Andreas.Beinert@ise.fraunhofer.de

1876-6102
Peer review by the scientific conference committee of SiliconPV 2017 under responsibility of PSE AG.
10.1016/j.egypro.2017.09.282

1. Introduction

With PV module degradation rates of up to 8% per year due to cracks in solar cells [4], the mechanical stability is a key factor for the PV module reliability. Hence it is essential to understand the origin of stresses within a PV module. So far an experimental method for measuring the stress in laminated cells is lacking. However, in microelectronics Raman spectroscopy is an established method for this purpose [1]. It allows the measurement of stress without a mechanical contact to the sample, additionally a spatial resolution of the mechanical stress is possible. In the field of photovoltaics (PV) Raman spectroscopy has been applied to solar cells so far [2, 3]. In this work we show that confocal Raman spectroscopy is capable of resolving thermomechanical stress in embedded solar cells within a PV laminate, measuring through the front glass.

2. Theory

The Raman effect describes the inelastic scattering of photons by matter. In silicon solar cells, the photons create lattice vibrations, so called phonons. If these phonons are not in the ground state when excited or do not relax to the ground state respectively, the frequency of the emitted photon ω_{em} is shifted relatively to the absorbed photon ω_{abs} by the frequency of the excited state Ω_{phon}: $\omega_{em} = \omega_{abs} \pm \Omega_{phon}$. Where minus denotes Raman (phonon relaxes to higher energy state, see fig. 1) and plus denotes anti-Raman scattering (phonon is in excited state, see fig. 1). Since the position of the Raman peak depends on the phonon energy levels, i.e. the lattice structure, the Raman peak position is a material property. Thus a change in the Raman peak correlates to lattice distortions, like deformation caused by mechanical stress. For the assumption of a uniaxial stress, the shift of the Raman peak position is converted into stress by a linear factor. This correlation and its dependency on various factors are examined in detail by Büchler *et al.* in [5]. In this work we use the conversion factor $\Sigma = -830 \pm 90$ MPa/(rel cm^{-1}) given in [5] for measurements from the sunny side of laminated solar cells.

The Raman peak position is subject to a statistical variation, which can be described by a Gauss-function, as shown in fig. 1 (b). We therefore use a high number of measurements to obtain reliable results.

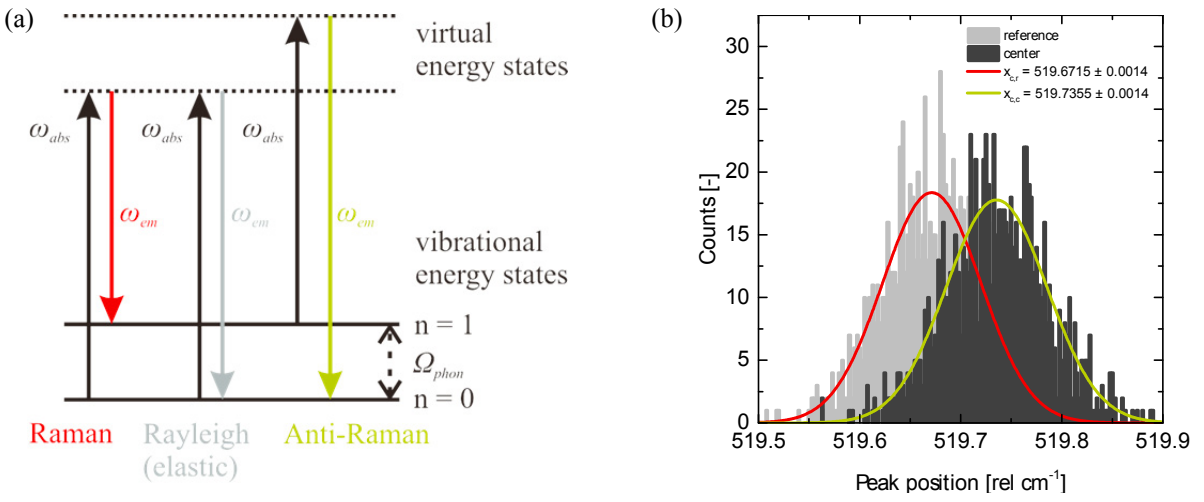

Fig. 1. (a) Schematic energy-level diagram of the Raman shift; ω_{abs}: frequency of absorbed photon, ω_{em}: frequency of emitted photon and Ω_{phon}: frequency of excited state; not to scale. (b) Peak positions of Raman measurements on a 1-cell mini-module (C-i) with a Gaussian fit to determine the mean position.

3. Method

We measure the thermomechanical stress in the solar cells after each module production step by Raman spectroscopy. In order to assess the obtained stress values, we simulate the soldering and lamination by a finite element model (FEM). The schematic of the module production process and the characterization steps are shown in fig. 2.

3.1. Raman measurements

In order to measure the thermomechanical stress from the manufacturing process by confocal Raman spectroscopy, twelve 1-cell mini-modules are manufactured using industrial processes. The material specifications are given in table 1. The stress is measured on the non-soldered solar cells (A), after soldering by an automatic stringer (B) and after lamination (C). In order to compare the obtained stresses with the value after lamination, we flatten the solar cell by covering it with a glass sheet. Additionally we measure the residual stress from the cell production by measuring the non-soldered cell also without a glass sheet (A-i). After each step we control the solar cells for cracks by electroluminescence imaging (EL), using a resolution of 2046 x 1900 pixels per cell.

Since the stress is proportional to a shift of the Raman peak in the order of magnitude of 0.01 rel cm^{-1}, the Raman spectroscopy represents a relative method which requires very precise measurements. Also the exact position of the Raman peak depends on various factors like temperature or the surface structure, as described in [5]. Therefore it is crucial to determine the reference peak precisely and under identical conditions as the actual measurements. Literature values cannot be considered. We use a location at the corner on the sunny side of the cell as the reference peak position, which is measured at each step. The actual measurement location is between two busbars in the center of the cell (compare fig. 3 (b)). We measure each position two times, while each measurement consists of 1000 single measurements with an integration time of 0.01 s using a 532 nm laser with a penetration depth of 1 µm. A Gauss-function is fitted to the obtained peak positions, as shown in fig. 1 (b). We then subtract the Gauss-peak value of the reference from the corresponding value of the measurement location in order to obtain the Raman peak shift. Finally we convert the weighted average peak shift of all cells into a stress value by the conversion factor Σ.

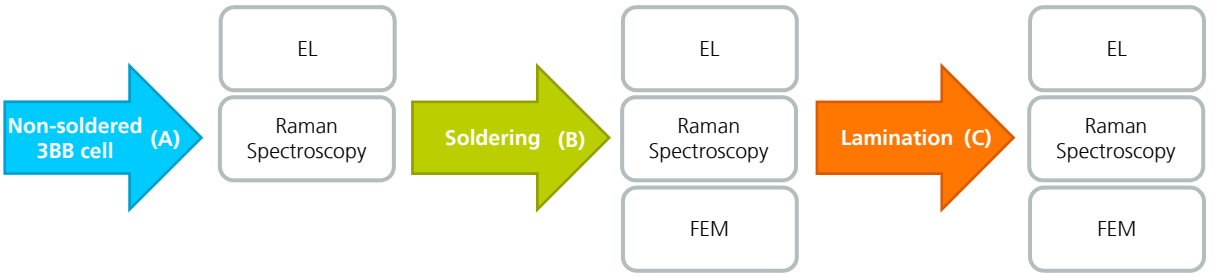

Fig. 2. Schematic flowchart of the conducted measurements and simulations after each module production step. EL: Electroluminescence imaging, FEM: Finite element modelling.

3.2. Finite element modelling

The soldering and lamination process of the 1-cell mini-module is simulated within one FEM model consisting of two computation steps. First the soldering of the solar cell is simulated by cooling down from the solder solidification temperature of 179 °C to ambient temperature. In the second step the lamination is simulated by cooling down from 160 °C to ambient temperature. Since the model is linear-elastic, the residual stress from soldering is reduced during the heating up process before the lamination. Therefore we transfer the stress tensor at lamination temperature, instead of ambient temperature, to the lamination model as the initial stress values.

We utilize the symmetry of the mini-module by simulating a quarter of it. The initial stress before soldering in the cells is set to zero, thereby we neglect stress originating from metallization or other cell production processes. The silver front busbars and rear side pads are considered, while the aluminum layer is not part of the model. We use linear-elastic and temperature dependent material models, which are shown in table 1. For the silicon solar cell an anisotropic material model is considered.

Table 1. Specifications of the mini-module materials with material properties used in the FEM model, *: provided by manufacturer.

Layer	Material	Dimension	Density (g/cm^3)	Youngs modulus (GPa)	Poisson's ratio (-)	CTE ($10^{-6}K^{-1}$)
Frontglass	soda-lime glass *	4 mm	2.5	70	0.2	8
Encapsulant	EVA [6]	400 µm	0.96	*T*-dep.	0.4	270
Solar Cell	Cz-Silicon [6–8]	156 x 156 x 0.180 mm^3	2.329	Elasticity matrix		*T*-dep.
Backsheet	TPT [6]	350 µm	2.52	3.5	0.29	50.4
Busbars	Silver [9]	145 x 1.35 x 0.014 mm^3	10.5	7	0.37	10
Ribbon	Copper [9, 10]	1.5 x 0.2 mm^2	8.7	70	0.35	17

4. Results

The shift of the Raman peak relative to the reference position along with the converted and simulated stress values are shown in table 2. In the following we will discuss the stress values only.

Due to the cooling down after the metallization process the aluminum layer on the rear side of the solar cell leads to a small bow of the non-soldered solar cell. For the corresponding initial compressive stress on the surface of the non-soldered cell (A-i) we obtain 9.3 ± 1.0 MPa. If the bow is flattened by placing a glass sheet on the solar cell, the compressive stress on the front side increases. According to the Raman measurements the flat cell (A-f) shows an 11 MPa higher compressive stress of 21 ± 2 MPa.

The cooling down from the solidification temperature of the solder during the soldering process further increases the compressive stress. We measure a compressive stress value on the flat cell (B-f) of 26 ± 3 MPa. Hence the soldering process induces additionally 5.5 MPa compressive stresses.

During the lamination process the solar cell is connected to the glass by the cross-linking of the EVA. Since this takes place at elevated temperatures, the solar cell is further compressed during the cooling down. After lamination (C-i) we measure 53 ± 6 MPa, which is an increase of 27 MPa.

From the FEM model of the soldering (B-m) process we obtain a compressive stress difference between the reference and the measurement position of 4 MPa. This difference increases in lamination (C-m) by 45 MPa to 49 MPa. In fig. 3 (b) the third principal stress σ_{III} on the front side of the solar cell after lamination, obtained from the FEM model, is shown along with the Raman measurements.

Table 2. Results of the Raman measurements and FEM modeling.

Cell process step	Raman peak shift [10^{-3} rel cm^{-1}]	Raman stress [MPa]	FEM stress [MPa]	FEM + initial stress [MPa]
Non-soldered (A-i)	11.24 ± 0.15	-9.3 ± 1.0	0 per def.	
Non-soldered flat (A-f)	24.8 ± 0.4	-21 ± 2	0 per def.	
Soldered flat (B-f)	31.4 ± 0.4	-26 ± 3	-4 (B-m)	-25
Laminated (C-i)	64 ± 2	-53 ± 6	-49 (C-m)	-69

Since the FEM simulation does not take the initial stress state into account, the obtained FEM values underestimate the Raman measurements. However if the initial stress state of the flat cell is taken into account the

FEM value increases to 25 MPa after soldering and 69 MPa after lamination. These values are depicted in fig. 3 (a) along with all Raman values. Considering the measured initial stress state, the values after soldering agree very well. For the stress after lamination the values deviate by 16 MPa. We assume that the FEM simulation overestimates the stress, due to the used linear elastic material model as indicated by Eitner *et al.* [6, 11]. However taking the nature of solar cells with the corresponding statistic scattering of the Raman peak into account, we consider the measured and simulated stress values to be in a good agreement.

The Raman stress measurements have three different uncertainties, namely on the measured Raman peak position, on the Gauss fit of the peak position distribution and on the conversion factor. The first two can be reduced by a high number of samples and measurements. Therefore the latter with about 11% [5] dominates the overall uncertainty.

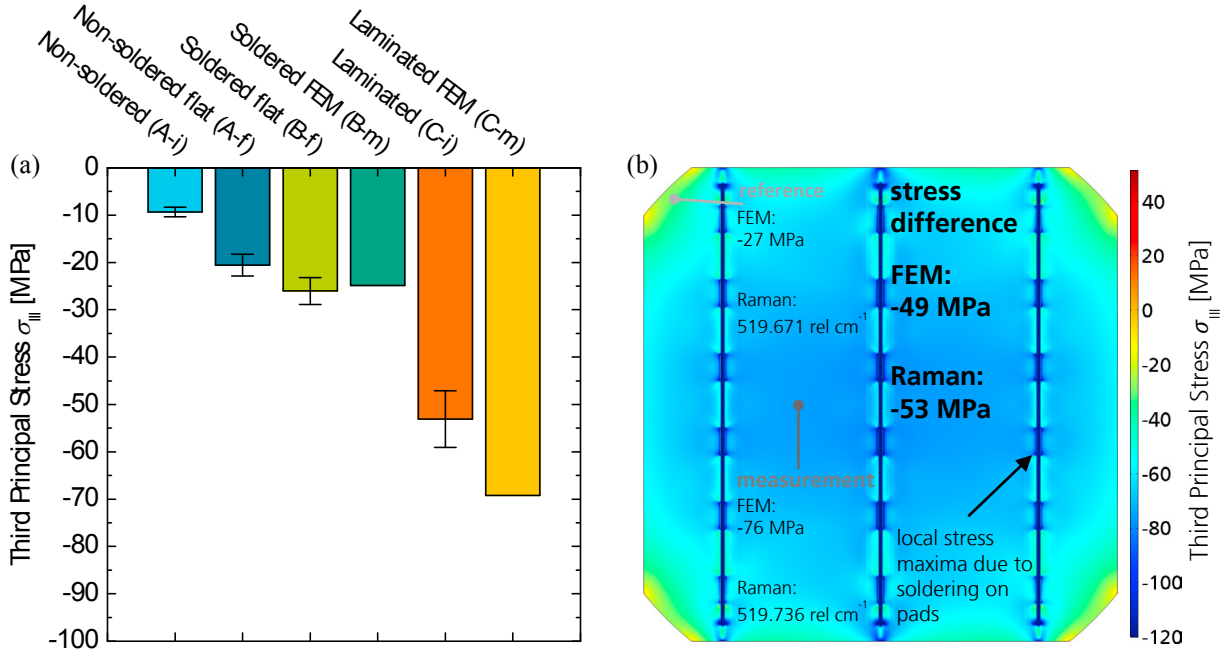

Fig. 3. (a) Third principal stress σ_{III} of all measurements and from the FEM model; the FEM values are a superposition of the initial stress of the flat non-soldered cell (B-f) and the FEM result. The uncertainty of the Raman values are depicted by the whiskers. (b) Results from the FEM model of lamination (C-m) on the cell surface with the corresponding Raman peak values at the measurement and reference position. Also the converted Raman peak shift with the corresponding simulated stress difference values are depicted in bold.

5. Conclusion

We demonstrate that confocal Raman spectroscopy can be applied on PV module level for measuring the thermomechanical stress in silicon solar cells through the front glass and encapsulant layer. In PV mini-modules we measure a build-up of compressive cell stress after the lamination of 53 ± 6 MPa. The same process is simulated by a FEM model leading to 69 MPa, including the measured initial stress state of the flat solar cell. Considering that the FEM model uses a linear elastic material model for EVA, these values are in good agreement. With an increase of the compressive stress in all module production steps, laminated solar cells are more stable against mechanical loads, than bare solar cells.

Acknowledgements

The authors like to thank Li Carlos Rendler for the fruitful discussions. This work has been supported by the Federal Ministry for Economic Affairs and Energy under the contract number 0325825B, acronym HERA and the Cusanuswerk by a PhD-scholarship.

References

[1] E. Anastassakis, A. Pinczuk, E. Burstein, F. H. Pollak, and M. Cardona, “Effect of static uniaxial stress on the Raman spectrum of silicon,” Solid State Communications, vol. 8, no. 2, pp. 133–138, 1970.
[2] W. Mühleisen, J. Schicker, L. Neumaier, C. Hirschl, N. Vollert, S. Seufzer, R. Battistutti, M. Pedevilla, J. Scheurer, M. Schwark, and T. Fischer, “Stress Measurements in Interconnected Solar Cells with Raman Spectroscopy,” in Proc. of the 31st European Photovoltaic Solar Energy Conference and Exihibition 2015, S. Rinck, N. Taylor, P. Helm, Ed, 2015, pp. 160–163.
[3] C. V. Schmid, “Schadensmechanismen bei Silizium-Solarzellen und Maßnahmen zur Festigkeitserhöhung,” Werkstoffwissenschaft und Werkstofftechnik, Aachen, 2010.
[4] M. Köntges, S. Altmann, T. Heimberg, U. Jahn, and K. A. Berger, “Mean Degradation Rates in PV Systems for Various Kinds of PV Module Failures,” in Proc. of the 32nd European Photovoltaic Solar Energy Conference and Exhibition, München: WIP, 2016, pp. 1435–1443.
[5] A. Büchler, A. J. Beinert, S. Kluska, V. Haueisen, F. D. Heinz, and M. C. Schubert, “Enabling stress determination on alkaline textured silicon using raman spectroscopy,” in Proceedings of the 7th International Conference on Crystalline Silicon Photovoltaics (SiliconPV 2017), 2017.
[6] U. Eitner, S. Kajari-Schroeder, M. Koentges, and H. Altenbach, “Thermal stress and strain of solar cells in photovoltaic modules,” in Advanced Structured Materials, vol. 15, Shell-like Structures: Non-classical Theories and Applications, H. Altenbach and V. A. Eremeyev, Eds, Berlin/Heidelberg: Springer, 2011.
[7] R. B. Roberts, “Thermal expansion reference data: silicon 300-850 K,” Journal of Physics D: Applied Physics, vol. 14, no. 10, pp. L163, 1981.
[8] R. B. Roberts, “Thermal expansion reference data: silicon 80-280K,” Journal of Physics D: Applied Physics, vol. 15, no. 9, pp. L119, 1982.
[9] S. Wiese, F. Kraemer, E. Peter, and J. Seib, “Mechanical problems of novel back contact solar modules,” in Thermal, Mechanical and Multi-Physics Simulation and Experiments in Microelectronics and Microsystems (EuroSimE), 2012 13th International Conference on, 2012, pp. 1–6.
[10] L. C. Rendler, A. Kraft, C. Ebert, S. Wiese, and U. Eitner, “Investigation of Thermomechanical Stress in Solar Cells with Multi Busbar Interconnection by Finite Element Modeling,” in Proc. of the 32nd European Photovoltaic Solar Energy Conference and Exhibition, München: WIP, 2016.
[11] U. Eitner, M. Pander, S. Kajari-Schröder, M. Köntges, and H. Altenbach, “Thermomechanics of PV Modules Including the Viscoelasticity of EVA,” in Proc. of the 26th European Photovoltaic Solar Energy Conference and Exhibition, 2011, pp. 3267–3269.